THE GEOLOGICAL SOCIETY OF AMERICA®

Late Cenozoic magmatic inflation, crustal thickening, and >2 km of surface uplift in central Tibet

Jian-Lin Chen[1,2,3]*, An Yin[3]*, Ji-Feng Xu[1,2], Yan-Hui Dong[4], and Zhi-Qiang Kang[5]

[1]State Key Laboratory of Isotope Geochemistry, Guangzhou Institute of Geochemistry, Chinese Academy of Sciences, Guangzhou 510640, China

[2]CAS (Chinese Academy of Sciences) Center for Excellence in Tibetan Plateau Earth Sciences, Beijing 100101, China

[3]Department of Earth, Planetary, and Space Sciences, University of California, Los Angeles, California 90095, USA

[4]Second Institute of Oceanography, State Oceanic Administration, Hangzhou 310012, China

[5]Guilin University of Technology, Guilin 541004, China

ABSTRACT

The high values of La/Yb (>15–20) obtained from late Eocene to Pliocene volcanic rocks of central Tibet indicate that source regions were in a thickened (>35 km) crust. The higher Neogene La/Yb values compared to lower Paleogene La/Yb values required continuous crustal thickening, as La/Yb values are proportional to crustal thickness. Although the Paleogene high La/Yb values can be explained by coeval thrusting, this mechanism is unable explain the Neogene higher La/Yb values because central Tibet is covered by undeformed flat-lying early Miocene strata. Here we correlate the temporal variation of Cenozoic volcanic geochemistry with the regional geology of central Tibet, which was part of a larger Eocene–Oligocene thrust belt and the related foreland basin. The Paleogene foreland basin was partitioned into the southern (Hoh Xil) and northern (Qaidam) subbasins by the Kunlun fault ca. 25–20 Ma. The two subbasins were at similar elevations at the time of their formation, but the southern basin, at ~5 km, is >2 km higher than the northern basin at ~2.8 km. Because the southern basin and the Paleogene thrust belt have been associated with Neogene volcanism and high La/Yb values, we suggest that the elevation difference between the two basins was induced by >15 km of magmatic inflation sourced from mantle melting. The magnitude of magmatic inflation is comparable to that of tectonic thickening in central Tibet, highlighting the important and often neglected role of syncollisional mantle melting and its induced magmatic inflation in constructing the thickened Tibetan crust.

INTRODUCTION

Although magmatic inflation plays an important role in crustal thickening of continental arcs (Lee et al., 2015; Perkins et al., 2016), how it affects collisional orogeny remains uncertain. This is exemplified by the existing crustal-thickening models of the Tibetan Plateau involving (1) constant-volume lithospheric shortening without mass exchange between crust and mantle (e.g., England and Houseman, 1986), (2) volume-reduction lithospheric shortening during which eclogitized mafic crust foundered into the mantle (e.g., Le Pichon et al., 1992), and (3) volume-gain lithospheric shortening coeval with magmatic inflation and thus further crustal thickening due to syncollisional mantle melting (e.g., Yin and Harrison, 2000). To address this issue we use regional geology and new geochemical data from Neogene volcanic rocks to show that central Tibet has been uplifted >2 km by >15 km of basaltic inflation since 25–20 Ma.

CENOZOIC VOLCANISM IN CENTRAL TIBET

Our study area is located in the northern Qiangtang terrane within the Eocene–Oligocene Fenghuo Shan thrust belt (Fig. 1A). Although Paleogene volcanism dominates the Qiangtang terrane, whereas Neogene–Quaternary volcanism dominates the Songpan-Ganzi terrane on the two sides of the Paleogene Fenghuo Shan thrust belt, our study area is unique in that it records nearly continuous volcanism from 35 to 4 Ma (Wei et al., 2004; Liu et al., 2004; Jin et al., 2010) (Fig. 1), allowing us to monitor the temporal evolution of the source regions. We obtained two new $^{40}Ar/^{39}Ar$ ages of ca. 6 Ma (Figs. DR1 and DR2 and Table DR1 in the GSA Data Repository[1]), similar to existing K-Ar ages of the same rocks (Fig. 1B). We analyzed the geochemistry of the dated rocks that show A-type granitoid composition, low Mg numbers from 22 to 51, and high values of high field strength elements (HFSE) (Fig. 2; Table DR2). An HFSE-enriched magma can be generated by crustal anatexis of tonalitic, granitic, and metasedimentary rocks (Patiño Douce, 1997), or fractionation of basaltic melt (e.g., Schmitt et al., 2000). The high SiO_2 (58–68 wt%), low MgO (≤2.65 wt%), Cr (≤ 92.2 ppm), and Ni (≤37.3 ppm) values, a lack of negative correlation between $^{87}Sr/^{86}Sr$ and 1/Sr, the positive correlation between La and La/Yb (or Sr and MgO), and the weak negative Eu anomalies all indicate a basaltic source (Baker et al., 1995; Rapp and Watson, 1995). This interpretation is further supported by the differences in large ion lithophile element concentrations (e.g., Ba and Sr) and incompatible element ratios (e.g., Ba/Rb or Rb/Sr) between our samples and the contemporary mantle-derived high-Mg potassic volcanic rocks (Fig. 2D; Fig. DR3). High CaO (≥1.78 wt%), V (≥44 ppm), and Cr (≥5.37 ppm) contents rule out metasediments or felsic granulite as the sole melting sources (e.g., Skjerlie and Johnston, 1992; King et al., 1997), whereas the Sr-Nd values between those of the Paleozoic ophiolites in Central Asia and the mafic granulite xenoliths in the Neogene volcanic rocks of central Tibet (Fig. 2C) require a juvenile basaltic source. Because La/Yb values are positively correlated to crustal thickness (e.g., Profeta et al., 2015; Farner and Lee, 2017), the higher Neogene La/Yb (or Sm/Yb and Gd/Yb) values than those of the Eocene volcanic rocks (Figs. 2D and 2E) indicate further crustal thickening after 25–20 Ma. Using normative quartz, albite, and orthoclase (Winkler, 1979), we estimate >10–15 kbar pressure for the Neogene source (Fig. DR4). The source temperature is estimated to be >900 °C (Fig. 2A) (Green and Pearson, 1986), consistent with the equilibrium temperatures of 800–1100 °C for the xenoliths in the Neogene volcanic rocks (Hacker et al., 2000; Lai et al., 2011) and required by the high HFSE concentrations (King et al., 1997). The drier and hotter Neogene source region (Fig. 2A) led to lower Neogene than Paleogene Sr/Y values, contrasting the typical positive correlation between Sr/Y values and crustal thickness for continental arcs (e.g., Chiaradia, 2015).

MAGMATIC INFLATION AND FORMATION OF THE TIBETAN PLATEAU

The high La/Yb value (>20) Eocene volcanism and implied thickened (> 35 km) crust

*E-mails: lzdxchen@gig.ac.cn; yin@epss.ucla.edu

[1]GSA Data Repository item 2018004, analytical methods and supplemental figures and tables, is available online at http://www.geosociety.org/datarepository/2018/ or on request from editing@geosociety.org.

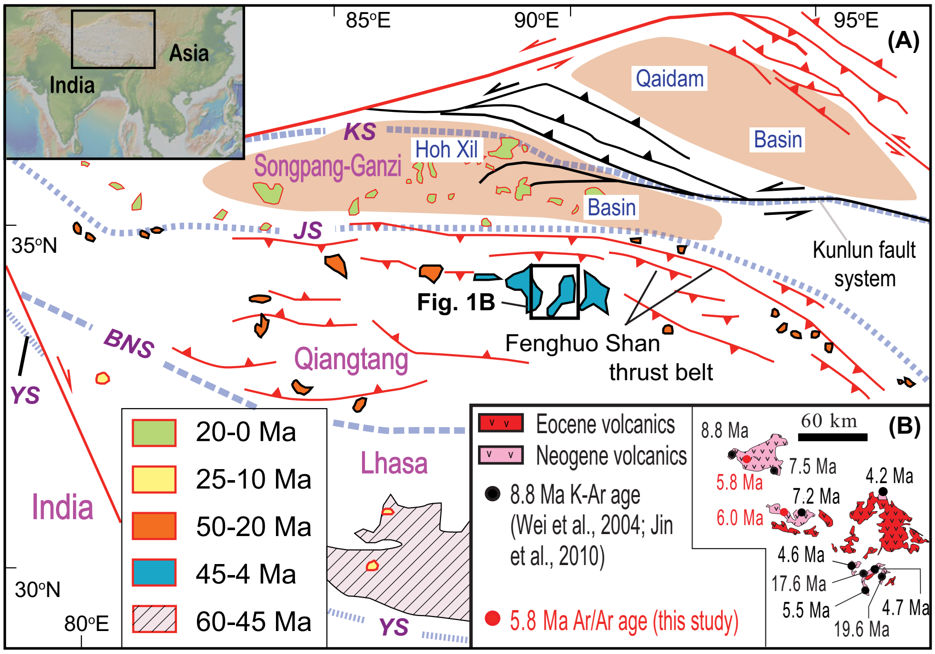

Figure 1. A: Tectonic map of central Tibet (after Yin et al., 2008); ages of Cenozoic volcanic rocks are from Wang et al. (2008), Jiang et al. (2009), and this study. See inset map for location. KS—Kunlun suture; JS—Jinsha suture; BNS—Bangong suture; YS—Yarlung-Zangbo suture. B: Age distribution of volcanic rocks in the study area.

Figure 2. A: TiO_2 versus SiO_2 plot based on Green and Pearson (1986). B: Age versus Nb plot. SG—Songpan-Ganzi terrane; NQT—northern Qiangtang terrane. C: $^{87}Sr/^{86}Sr_{(0)}$ versus $\varepsilon_{Nd(0)}$ plot. MORB—mid-oceanic ridge basalt; HFSE—high field strength elements. D: La/Yb versus Yb plot based on Kay and Mpodpzos (2001) and Haschke et al. (2002). E: Gd/Yb versus age plots (inset in D). See Table DR2 (see footnote 1) for data source. Paleo-Asia MORB data are from Liu et al. (2014). NQT—northern Qiangtang terrane; SQT—southern Qiangtang terrane; SG—Songpan-Ganzi terrane.

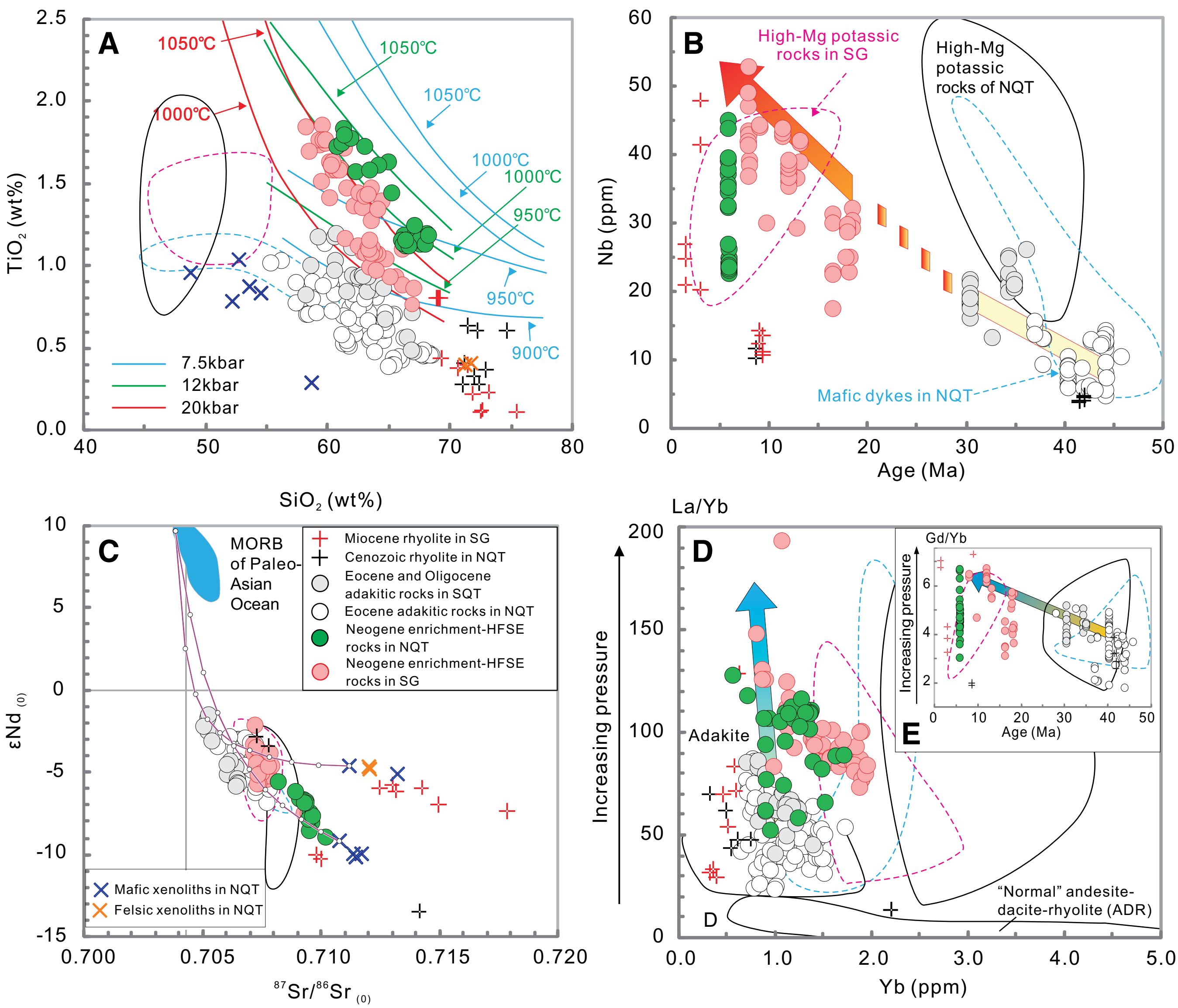

(Wang et al., 2008) in northern Qiangtang of central Tibet can be attributed to coeval intraplateau thrusting (e.g., Yin, 2010). However, the even higher Neogene La/Yb values cannot be related to the same mechanism, because central Tibet is covered by flat-lying early Miocene lacustrine strata, indicating that thrusting had ended by that time (Yin et al., 2008). The modern Hoh Xil basin was part of the much larger Eocene–Oligocene foreland basin of the Fenghuo Shan thrust belt. The foreland basin was partitioned into the northern and southern subbasins by the Kunlun fault ca. 25–20 Ma (Yin et al., 2008) (Figs. 1 and 3). The two subbasins were essentially at the elevation at the end of the Paleogene thrusting, similar to the modern Indus and Ganges Plains in the Himalayan foreland. However, the southern subbasin (Hoh Xil) at ~5 km is currently >2 km higher than the northern subbasin (Qaidam) at ~2.9–2.7 km, which was attributed to possible southward lower crustal injection (Yin et al., 2008) or mantle upwelling in the sense of Molnar et al. (1993) (see Yin, 2010). Because lower crustal flow does not explain Neogene volcanism, we attribute the surface uplift of the southern subbasin to basaltic underplating through mantle melting (Fig. 3). This model is consistent with the lack of Cenozoic volcanism in the northern subbasin that is at a lower elevation north of the Kunlun fault. The northern Qiangtang terrane and the Hoh Xil basin are bounded by the Fenghuo Shan thrust belt, which ceased motion in the late Oligocene; therefore, uplift of the Hoh Xil basin must have been coupled with the uplift of the northern Qiangtang terrane, where our samples were collected (Fig. 1).

Quantifying the magnitude of magmatic inflation depends on how the crust is compensated, which cannot be determined uniquely. This is because the estimated crustal thickness of central Tibet varies drastically, from ~60 km based on dense-array broad-band seismology (Tseng et al., 2009) to >75 km based on multiscale gravimetric modeling (Xu et al., 2017). We consider the simplest case that central Tibet is under Airy isostasy and its crust has been thickened from 40 to 70 km during the Cenozoic India-Asia collision. This yields ~15 km of magmatic thickening (dH) as $dh/dH = (1 - \rho_c/\rho_m)$ (Lee et al., 2015), where surface uplift, dh = 2 km, crustal density, ρ_c = 2.8 g/cm^3, and mantle density, ρ_m = 3.2 g/cm^3. We acknowledge that this estimate could vary if the current elevation is partially supported by an upwelling mantle with our estimate as an upper bound, or dragged down by eclogitized crustal material with our estimate as a lower bound (e.g., Lee et al., 2015). Our assumed 70 km crustal thickness and the estimated 15 km magmatic inflation in the Neogene require central Tibet to have been thickened by ~15 km in the Paleogene; this can be attributed to the combined effect of Fenghuo Shan thrusting and magmatic inflation. Together with the inference that magmatic underplating has also contributed to Cenozoic thickening of the southern Tibet crust (Yin and Harrison, 2000; Zhu et al., 2017), mantle melting may have played an equal or even more dominant role than tectonic deformation in constructing the thickened Tibetan crust. Our results imply that syncollisional magmatism from mantle melting is an important process of collisional orogeny, which has not been considered in the state of the art geodynamic models (e.g., Sternai et al., 2016).

ACKNOWLEDGMENTS

We are thankful for constructive comments by the anonymous reviewers and funding support by the Strategic Priority Research Program (B) of the Chinese Academy of Sciences (XDB03010300), Chinese National Key Research and Development Program (2016YFC0600305), Chinese Major State Basic Research Program (2015CB452602), Chinese National Science Foundation (41373030, 41573024), and U.S. National Science Foundation Continental Dynamics Program. We also thank James Schmitt for the encouragement, detailed editing, and constructive suggestions throughout the preparation of this manuscript. This is contribution No. IS-2441of GIGCAS (the Guangzhou Institute of Geochemistry, Chinese Academy of Sciences).

REFERENCES CITED

Baker, M.B., Hischmann, M.M., Ghiorso, M.S., and Stolper, E.M., 1995, Compositions of near-solidus peridotite melts from experiments and thermodynamic calculations: Nature, v. 375, p. 308–311, https://doi.org/10.1038/375308a0.

Chiaradia, M., 2015, Crustal thickness control on Sr/Y signatures of recent arc magmas: An Earth scale perspective: Scientific Reports, v. 5, 8115, https://doi.org/10.1038/srep08115.

England, P., and Houseman, G., 1986, Finite strain calculations of continental deformation 2. Comparison with the India-Asia collision zone: Journal of Geophysical Research, v. 91, p. 3664–3676, https://doi.org/10.1029/JB091iB03p03664.

Farner, M.J., and Lee, C.T.A., 2017, Effects of crustal thickness on magmatic differentiation in subduction zone volcanism: A global study: Earth and Planetary Science Letters, v. 470, p. 96–107, https://doi.org/10.1016/j.epsl.2017.04.025.

Green, T.H., and Pearson, N.J., 1986, Ti-rich accessory phase saturation in hydrous mafic-felsic compositions at high P, T: Chemical Geology, v. 54, p. 185–201, https://doi.org/10.1016/0009-2541(86)90136-1.

Hacker, B., Gnos, E., Ratschbacher, L., Grove, M., McWilliams, M., Sobolev, S.V., Jiang, W., and Wu, Z.H., 2000, Hot and dry deep crustal xenoliths from Tibet: Science, v. 287, p. 2463–2466, https://doi.org/10.1126/science.287.5462.2463.

Haschke, M., Siebel, W., Günther, A., and Scheuber, E., 2002, Repeated crustal thickening and recycling during the Andean orogeny in north Chile (21°–26°S): Journal of Geophysical Research, v. 107, p. 426–433, https://doi.org/10.1029/2001JB000328.

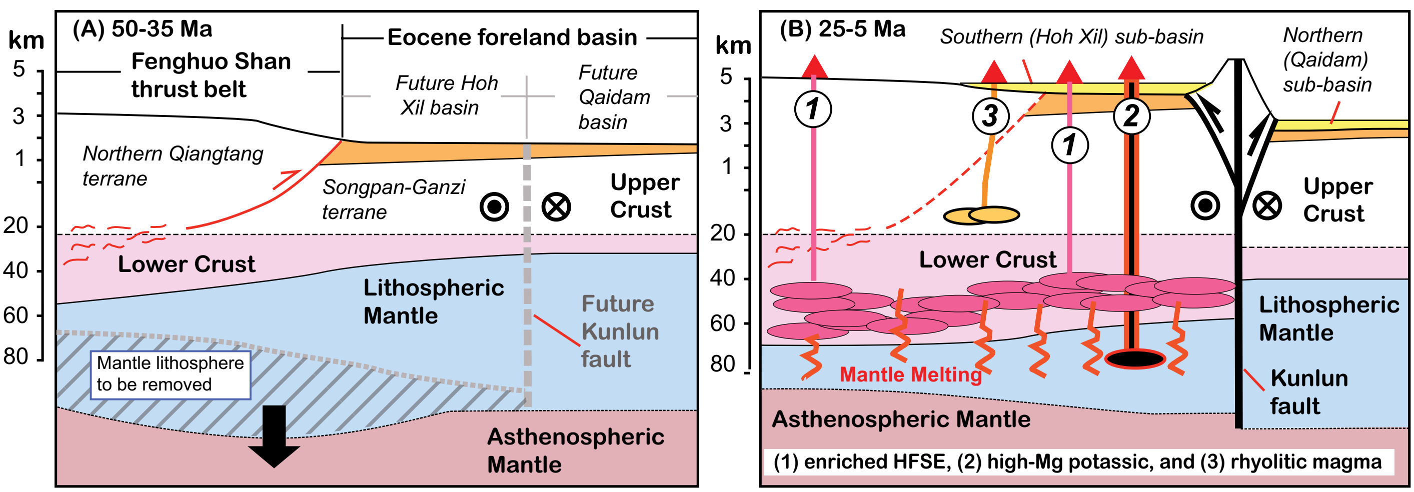

Figure 3. Tectonic model of crustal thickening and surface uplift as a result of Paleogene crustal shortening and Neogene magmatic inflation. A: 50–35 Ma. Development of the Fenghuo Shan thrust and foreland basin in central Tibet. B: Transpression along the Kunlun fault system partitioned the Paleogene foreland into the northern Qaidam basin and southern Hoh Xil basin at 25–20 Ma. This was followed by magmatic inflation due to mantle melting across the Hoh Xil area, raising its surface by >2 km relative to that of the Qaidam basin. HFSE—high field strength elements.

Jiang, D., Liu, J., and Ding, L., 2009, Geochemistry and petrogenesis of Cenozoic potassic volcanic rocks in the Hoh Xil area, northern Tibet plateau: Yanshi Xuebao, v. 24, p. 279–290.

Jin, C., Zhu, T., Zhou, B., and Yu, Y., 2010, Geochemical features of Neogene volcanic rocks in the Shawotan-Hongyuquan area of northern Qiangtang in Tibet and their tectonic implication: Geology and Exploration, v. 46, p. 1061–1070.

Kay, S.M., and Mpodpzos, C., 2001, Central Andean ore deposits linked to evolving shallow subduction systems and thickening crust: GSA Today, v. 11, p. 4–9, https://doi.org/10.1130/1052-5173(2001)011<0004:CAODLT>2.0.CO;2.

King, P.L., White, A.J.R., Chappell, B.W., and Allen, C.M., 1997, A-type granites form the Lachlan fold belt, southeastern Australia: Journal of Petrology, v. 38, p. 371–391, https://doi.org/10.1093/petroj/38.3.371.

Lai, S., Qin, J., and Grapes, R., 2011, Petrochemistry of the granulite xenoliths from Cenozoic Qiangtang volcanic field, northern Tibetan Plateau: Implication for lower crust composition and the genesis of volcanism: International Geology Review, v. 53, p. 926–945, https://doi.org/10.1080/00206810903334914.

Lee, C.T.A., Thurner, S., Paterson, S., and Cao, W., 2015, The rise and fall of continental arcs: Interplays between magmatism, uplift, weathering, and climate: Earth and Planetary Science Letters, v. 425, p. 105–119, https://doi.org/10.1016/j.epsl.2015.05.045.

Le Pichon, X., Fournier, M., and Jolivet, L., 1992, Kinematics, topography, shortening, and extrusion in the India-Eurasia collision: Tectonics, v. 11, p. 1085–1098, https://doi.org/10.1029/92TC01566.

Liu, H., Xia, B., Deng, W., Zhang, Y., 2004, Study of ^{40}Ar-^{39}Ar and K-Ar dating on the high-K volcanic rock from Bamaoqiongzong to Qiangbaqian in northern Tibet: Journal of Mineralogy and Petrology, v. 24, p. 71–75.

Liu, X., Xu, J., Castillo, P.R., Xiao, W., Shi, Y., Feng, Z., and Guo, L., 2014, The Dupal isotopic anomaly in the southern paleo-Asian Ocean: Nd-Pb isotope evidence from ophiolites in the northwest China: Lithos, v. 189, p. 185–200, https://doi.org/10.1016/j.lithos.2013.08.020.

Molnar, P., England, P., and Martinod, J., 1993, Mantle dynamics, the uplift of the Tibetan Plateau, and the Indian monsoon: Reviews of Geophysics, v. 31, p. 357–396, https://doi.org/10.1029/93RG02030.

Patiño Douce, A.E., 1997, Generation of metaluminous A-type granites by low-pressure melting of calc-alkaline granitoids: Geology, v. 25, p. 743–746, https://doi.org/10.1130/0091-7613(1997)025<0743:GOMATG>2.3.CO;2.

Perkins, J.P., Ward, K.M., De Silva, S.L., Zandt, G., Beck, S.L., and Finnegan, N.J., 2016, Surface uplift in the Central Andes driven by growth of the Altiplano Puna magma body: Nature Communications, v. 7, 13185, https://doi.org/10.1038/ncomms13185.

Profeta, L., Ducea, M.N., Chapman, J.B., Paterson, S.R., Gonzales, S.M.H., Kirsch, M., Petrescu, L., and DeCelles, P.G., 2015, Quantifying crustal thickness over time in magmatic arcs: Scientific Reports, v. 5, 17786, https://doi.org/10.1038/srep17786.

Rapp, R.P., and Watson, E.B., 1995, Dehydration melting of metabasalt at 8–32 kbar: Implications for continental growth and crust-mantle recycling: Journal of Petrology, v. 36, p. 891–931, https://doi.org/10.1093/petrology/36.4.891.

Schmitt, A.K., Emmermann, R., Trumbull, R.B., Buhn, B., and Henjes Kunst, F., 2000, Petrogenesis and ^{40}Ar/^{39}Ar geochronology of the Brandberg Complex, Namibia: Evidence for a major mantle contribution in metaluminous and peralkaline granites: Journal of Petrology, v. 41, p. 1207–1239, https://doi.org/10.1093/petrology/41.8.1207.

Skjerlie, K.P., and Johnston, A.D., 1992, Vapor-absent melting at 10 kbar of a biotite- and amphibole-bearing tonalitic gneiss: Implications for the generation of A-type granites: Geology, v. 20, p. 263–266, https://doi.org/10.1130/0091-7613(1992)020<0263:VAMAKO>2.3.CO;2.

Sternai, P., Avouac, J.P., Jolivet, L., Faccenna, C., Gerya, T., Becker, T.W., and Menant, A., 2016, On the influence of the asthenospheric flow on the tectonics and topography at a collision-subduction transition zones: Comparison with the eastern Tibetan margin: Journal of Geodynamics, v. 100, p. 184–197, https://doi.org/10.1016/j.jog.2016.02.009.

Tseng, T.L., Chen, W.P., and Nowack, R.L., 2009, Northward thinning of Tibetan crust revealed by virtual seismic profiles: Geophysical Research Letters, v. 36, https://doi.org/10.1029/2009GL040457.

Wang, Q., et al., 2008, Eocene melting of subducting continental crust and early uplifting of central Tibet: Evidence from central-western Qiangtang high-K calc-alkaline andesites, dacites and rhyolites: Earth and Planetary Science Letters, v. 272, p. 158–171, https://doi.org/10.1016/j.epsl.2008.04.034.

Wei, J., Wang, J., and Niu, Z., 2004, The Cenozoic volcanic rocks from the Chibuzhang Lake area in the Qiangtang area: Sedimentary Geology and Tethyan Geology, v. 24, p. 16–21.

Winkler, H.G.F., 1979, Petrogenesis of metamorphic rocks: New York, Springer-Verlag. 348 p., https://doi.org/10.1007/978-1-4757-4215-2.

Xu, C., Liu, Z., Luo, Z., Wu, Y., and Wang, H., 2017, Moho topography of the Tibetan Plateau using multi-scale gravity analysis and its tectonic implications: Journal of Asian Earth Sciences, v. 138, p. 378–386.

Yin, A., 2010, Cenozoic tectonic evolution of Asia: A preliminary synthesis: Tectonophysics, v. 488, p. 293–325, https://doi.org/10.1016/j.tecto.2009.06.002.

Yin, A., and Harrison, T.M., 2000, Geologic evolution of the Himalayan-Tibetan orogen: Annual Review of Earth and Planetary Sciences, v. 28, p. 211–280, https://doi.org/10.1146/annurev.earth.28.1.211.

Yin, A., Dang, Y., Zhang, M., Chen, X., and McRivette, M.W., 2008, Cenozoic tectonic evolution of the Qaidam basin and its surrounding regions (Part 3): Structural geology, sedimentation, and regional tectonic reconstruction: Geological Society of America Bulletin, v. 120, p. 847–876, https://doi.org/10.1130/B26232.1.

Zhu, D.C., Wang, Q., Cawood, P.A., Zhao, Z.D., and Mo, X.X., 2017, Raising the Gangdese Mountains in southern Tibet: Journal of Geophysical Research, v. 122, p. 214–223, https://doi.org/10.1002/2016JB013508.

Manuscript received 27 October 2016
Revised manuscript received 15 September 2017
Manuscript accepted 19 September 2017

Printed in USA